

# Multi-Layer Perceptron Decomposition Architecture for Mobile IoT Indoor Positioning

Erdem Çakan

*Department of Electrical and Electronics Engineering  
Yaşar University  
Izmir, Turkey  
cakanerdem5@gmail.com*

Aral Şahin

*Department of Electrical and Electronics Engineering  
Ege University  
Izmir, Turkey  
aralsahin4@gmail.com*

Mert Nakip

*Institute of Theoretical and Applied Informatics  
Polish Academy of Sciences (PAN)  
Gliwice, Poland  
mnakip@iitis.pl*

Volkan Rodoplu

*Department of Electrical and Electronics Engineering  
Yaşar University  
Izmir, Turkey  
volkan.rodoplu@yasar.edu.tr*

**Abstract**—We develop a Multi-Layer Perceptron (MLP) Decomposition architecture for mobile Internet Things (IoT) indoor positioning. We demonstrate the performance of our architecture on an indoor system that utilizes ultra-wideband (UWB) positioning. Our architecture outperforms the following benchmark processing techniques on the same data: MLP, Linear Regression, Ridge Regression, Support Vector Regression, and the Least Squares Method for indoor positioning. The results show that our architecture can significantly advance the positioning accuracy of indoor positioning systems and enable indoor applications such as navigation, proximity marketing, asset tracking, collision avoidance, and social distancing.

**Index Terms**—indoor positioning, Multi-Layer Perceptron (MLP), Artificial Intelligence (AI), machine learning (ML), Ultra-wideband (UWB), Internet of Things (IoT)

## I. INTRODUCTION

Indoor positioning (IP) [1] is one of the significant problems that must be solved in order to enable a variety of applications for the mobile Internet of Things (IoT) including navigation, proximity marketing, asset tracking, collision avoidance, and social distancing. While significant advances have been made in this area over the past decade [2], IP systems still suffer from low positioning accuracy due to Non-Line of Sight (NLoS) scenarios. Ultra-Wideband (UWB) has emerged as one of the key methods in achieving high positioning accuracy; however, it can still suffer from significant degradation in performance due to multipath components in the wireless environment. As a result, novel signal and information processing techniques are required in order to achieve robust positioning accuracy in indoor environments that have multiple obstacles.

Artificial Intelligence (AI) techniques hold much promise to process information in IP systems [3]. In this paper, we develop a novel architecture based on AI, which we call “Multi-Layer Perceptron (MLP) Decomposition” for mobile IoT indoor positioning. In our architecture, in the first stage, a

bank of MLPs process the position and distance information from each anchor. In the second stage, the outputs of the bank of MLPs are fed into a main MLP block. While decomposition of MLPs into multiple stages has been used in the Machine Learning (ML) literature [4]–[6], to the best of the authors’ knowledge, this is the first work that uses a design based on MLP decomposition for indoor positioning.

We demonstrate the performance of our architecture on actual data collected in an indoor environment with multiple obstacles. We show that our architecture outperforms all of the following benchmark processing techniques with respect to mean positioning error on the same data, when all of these techniques have been optimized: MLP, Linear Regression, Ridge Regression, Support Vector Regression and the Least Squares Method for indoor positioning [7]. These results imply that our architecture can significantly advance the positioning accuracy of existing indoor positioning systems and enable mobile IoT indoor applications that require high positioning performance.

The rest of this paper is organized as follows: In Section II, we compare our work against the past work in this area. In Section III, we describe our MLP Decomposition architecture. In Section IV, we present our results on the positioning performance as well as the computation time. In Section V, we present our conclusions.

## II. RELATED WORK

In this section, we describe the relationship of this work to the literature in four categories: (1) We contrast our work against those that utilize lower-precision indoor positioning technologies. (2) We explain the differences between our work and high-precision indoor positioning technologies. (3) We contrast our work with alternative processing technologies that do not utilize AI. (4) We describe the differences between our work and other processing techniques that utilize AI for indoor positioning.

First, in regard to articles in the relatively low-precision indoor positioning technology, Reference [8] achieves a positioning error of 50 cm by using RSSI data from BLE devices. In [9], a positioning error of 37 cm was achieved by using a 24-GHz radar. In [10], an Ultrasonic Time of Flight (ToF) approach was utilized to obtain a positioning error of 31 cm. In contrast with these articles, in our demonstrations in this paper, we use UWB technology in conjunction with our MLP decomposition architecture in order to achieve much higher positioning accuracy.

Second, in the category of high-precision indoor positioning technologies, References [11], [12], and [13] (as cited by [14]) achieve a positioning error of 20 cm, 5 cm, 3.3 cm, respectively; however, the high-precision LIDAR technology was used in achieving such low error. In [15]–[18], by using the Visible Light Positioning (VLP), positioning errors of 17 cm, 7 cm, 1 cm, 0.82 cm, respectively, were obtained in a small experimental area without any obstacles between the light sources and the object. Even though these articles achieve very low positioning error, the high performance obtained is due to the underlying technology utilized. In contrast, in this paper, we develop a *processing* technique that improves the performance of the underlying technology.

Third, we discuss the past work in the category of non-AI-based processing techniques for indoor positioning, in particular when UWB is used as the underlying technology: In [19], an UWB positioning system for tracking customer pathway achieved a 11 cm positioning error in a small retail shop-like space with rows of shelves. In [20], a Simultaneous Calibration and Localization (SCAL) algorithm framework achieves a 25 cm and a 24 cm positioning error for target and beacon positioning, respectively, in an indoor supermarket passageway. In [21] and [22], a federated and standard Extended Finite Impulse Response (EFIR) filter achieved 36 cm and 18 cm positioning errors, respectively, for UWB positioning in an empty indoor experiment area of a university building. In [23] (as cited by [14]) and [24], both works used UWB technology in their approaches and achieved 29 cm and 23 cm positioning errors, respectively. In contrast with these existing processing techniques for UWB indoor positioning systems, in this paper, we develop a novel processing technique based on AI.

Fourth, we address the references in the category of AI-based processing techniques for indoor positioning: In [25], an MLP model is used for learning the relationship between the input and the output of an indoor positioning processing system and the results are compared with the  $k$ -Nearest Neighbor ( $k$ -NN) algorithm. In [26], a Kalman filter based on Bayesian Filtering is used to overcome signal propagation in complex environments. In [27], temporal fluctuations of radio signals are analyzed; strong and weak radio wave groups are processed via the  $k$ -means clustering algorithm. In [28], a combination of a Convolutional Neural Network (CNN) and Long Short-Term Memory (LSTM) are used respectively to extract features and to classify UWB data. In [29], existing machine learning algorithms are compared in terms of processing time and accuracy by utilizing an RSS fingerprint

dataset which is taken by Wi-Fi devices in a multi-room environment. In [30], an online independent support vector machine classification method is used in conjunction with the RSSI of Wi-Fi signals, thereby reducing the estimation error. Our 2-stage MLP Decomposition technique is distinct from all of the above AI-based processing techniques for indoor positioning and achieves high positioning accuracy.

### III. MLP DECOMPOSITION ARCHITECTURE FOR INDOOR POSITIONING

In this section, we describe our novel MLP Decomposition architecture for indoor positioning.

We first state the assumptions that underlie the design of our architecture: We assume an indoor positioning system that has been deployed over a region  $R$ . We focus on a system with  $n$  anchors and 1 tag, where the tag corresponds to the mobile device whose position we wish to determine.<sup>1</sup> We let  $T$  denote the tag, and let  $A_i$  denote the  $i$ th anchor, where  $i \in \{1, \dots, n\}$ . We let  $d_i$  denote the distance between  $A_i$  and  $T$ . Furthermore, we let  $x_{A_i}$  and  $y_{A_i}$  denote the  $x$  and  $y$  coordinates of the position of  $A_i$ .<sup>2</sup> (Note that these coordinates do not change over time in our system; only  $d_i$  may change over time if the tag moves around.)

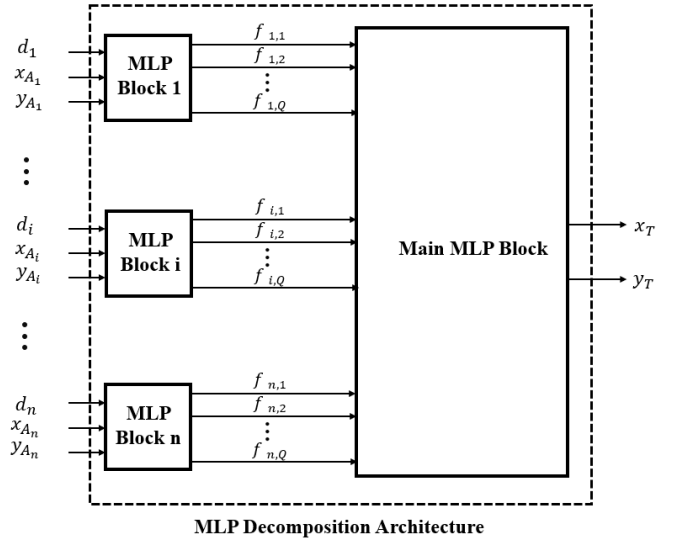


Fig. 1. MLP Decomposition Architecture for Indoor Positioning

In Fig. 1, we display our MLP Decomposition architecture, which is an end-to-end trainable neural network architecture.<sup>3</sup> In this architecture, the Main MLP Block combines the outputs of  $n$  MLP models, each of which is for a single anchor. The main idea behind this architecture is to achieve data fusion

<sup>1</sup>We focus on a system with a single tag. Once we develop our method, it can be applied to each tag in a system that has many tags.

<sup>2</sup>We model a position only on the two-dimensional plane in this paper; we do not consider the position in three-dimensional space.

<sup>3</sup>A neural network architecture is said to be end-to-end trainable if the entire architecture is trained together. In this case, we emphasize that each MLP block in the first stage and the Main MLP block in the second stage are *not* trained separately.

in two stages: In the first stage, each MLP Block  $i$  fuses the distance  $d_i$  for the  $T - A_i$  pair with  $x_{A_i}$  and  $y_{A_i}$  (which are inputs to this MLP block) in order to produce a set of features  $\{\{f_{i,q}\}_{q \in \{1, \dots, Q\}}\}$ , where  $f_{i,q}$  is the  $q$ th output of the MLP Block  $i$ . In the second stage, the Main MLP Block fuses these sets of features (received as the outputs of the MLP blocks in the first stage) in order to produce  $(x_T, y_T)$ , namely the estimate of the current position of tag  $T$ .

Each MLP Block  $i$  is comprised of  $L$  hidden layers and an output layer (which is the  $L + 1$ st layer). Each layer  $l \in \{1, \dots, L + 1\}$  contains  $H_l$  neurons, each of which is defined by its connection weights, its bias parameter and activation function. The Main MLP Block in Fig. 1 is comprised of  $L_{\text{main}}$  hidden layers and an output layer. The output layer consists of 2 neurons that correspond to  $x_T$  and  $y_T$ . Each hidden layer  $l \in \{1, \dots, L_{\text{main}}\}$  contains  $H_l^{\text{main}}$  neurons. The parameters of each neuron in the Main MLP Block are its connection weights, its bias parameter and activation function.

#### IV. RESULTS

In this section, we demonstrate the empirical results for our MLP decomposition architecture in an UWB system. We compare the results with alternative techniques that process the same set of positioning data. We show that our architecture outperforms all of the alternative techniques studied in our experimental set-up.

##### A. Experimental Setup

In this section, we aim to explain how we have obtained our dataset. We emphasize that all of our results are based on actual indoor positioning data that have been collected by an UWB system. Our system uses the anchors and the tag in the Decawave DWM1001 module [31].

The deployment area for the anchors and the tag in our experimental study is a furnished living room of a 3 m  $\times$  2.1 m apartment. We emphasize that this environment has a rich multipath profile; since the UWB signal has a very wide bandwidth, the channel seen by the UWB signal is highly frequency-selective. Thus, this constitutes a scenario with many NLoS components in addition to the LoS component, which was present most of the time.

In our experiment, the number of anchors selected was  $n = 4$ . The anchors were located close to the four corners of the room. The room was divided into a two-dimensional grid of 15 cm  $\times$  15 cm cells. In our experiment, the tag visited the cell vertices in this grid exactly once. We took 5 distance measurements, spaced at 4 second intervals, at all of the anchors for each visit of the tag to a vertex.

##### B. Parameter Tuning and Training

In this section, we explain the internal architecture of all of the techniques that we use in our experiments. We compare the indoor positioning accuracy of our MLP Decomposition architecture against those of the following techniques: MLP, Linear Regression, Ridge Regression, Support Vector Regression and the Least Squares Method for indoor positioning [7].

The training and optimization of all of these techniques were performed in Python on Google Colab platform, except for the Least Squares Method, which was performed in MATLAB.

The set of inputs to each of the above models was  $(x_{A_i}, y_{A_i})$  and  $d_i$ , except for the Least Squares Method whose input was only the  $d_i$ , where  $i \in \{1, \dots, n\}$ . We applied Max Normalization in order to normalize the values of distances and the anchor coordinates to the range  $[0, 1]$ .

Table I displays the optimized configurations for the techniques under examination. The first row of this table shows the end-to-end optimized configuration of the MLP decomposition architecture. (Recall that the internal architecture of each MLP block in the first stage of Fig. 1 is identical; hence, the table shows the resulting configurations of the MLP block and the Main MLP block in this figure.) In our notation,  $[H_1, \dots, H_L]$  is a vector whose  $l$ th entry  $H_l$  is the number of neurons in neural layer  $l$ . We use this notation in the table in order to show the number of neurons in each hidden layer for the MLP Decomposition architecture on the first row and for the MLP on the second row of this table. In addition, we give the configurations of the remaining techniques in the rest of this table.

TABLE I  
OPTIMIZED CONFIGURATIONS FOR THE TECHNIQUES UNDER EXAMINATION

Model Type	Parameters
MLP Decomposition	MLP Block: [130 148 74] Main MLP Block: [68 88 24]
MLP	[126 118 36]
Linear Regression	-
Ridge Regression	$\alpha = 0.01$
SVR-1	Kernel: Linear
SVR-2	Kernel: Radial Basis Function (RBF)
SVR-3	Kernel: Polynomial
SVR-4	Kernel: Sigmoid
Least Squares Method	-

1) *MLP Decomposition Architecture*: We set the activation function of each layer of the MLP Decomposition architecture to Tangent Hyperbolic ( $\tanh$ ). We used the Keras Application Programming Interface, which is a deep learning interface of the TensorFlow platform of Python. Furthermore, we employed Adam in order to optimize the learning process and used Mean Squared Error (MSE) as our error metric.

We used the following random search algorithm in order to arrive at a local optimal MLP Decomposition architecture: Consider the set  $S$  that is comprised of all of the integers from 10 to 150 in increments of 2. We generate 100 MLP Decomposition architectures independently by applying the following procedure to generate each such architecture.

*Procedure*: We pick 6 elements at random successively from this set  $S$  and denote the resulting sequence by  $\langle U \rangle$ . We set the number of hidden layers  $L$  in each MLP block in the first stage in Fig. 1 to 3. Then, we set the number of neurons  $H_l$  in the  $l$ th layer of each MLP block as  $H_l = U[l]$ , for each  $l \in \{1, 2, 3\}$ . We set the number of hidden layers  $L_{\text{main}}$  in the Main MLP block to 3. We set the number of neurons in

the  $l$ th layer of each MLP block as  $H_l^{\text{main}} = U[l]$  for each  $l \in \{4, 5, 6\}$ .

We split our dataset into the training and test sets as 85% and 15%, respectively. We train and test each of the 100 MLP Decomposition architectures generated above on the same train and test sets. Throughout this paper, we define the ‘‘positioning error’’ as the difference in Euclidean distance between the actual position and the estimated position on the two-dimensional plane. Our optimized MLP architecture is defined as the MLP Decomposition architecture that has the lowest mean positioning error for the test set across these 100 MLP Decomposition architectures.

### C. Performance Comparison

In Table II, we compare the performance of all of the techniques in Table I by using 10-fold cross-validation. We measure the performance with respect to three metrics: (1) Mean positioning error; (2) Standard deviation (STD) of positioning errors; (3) Coefficient of determination  $R^2$ , which takes values on the interval  $[0, 1]$ .

TABLE II  
10-FOLD CROSS-VALIDATION PERFORMANCE RESULTS

Model Type	Mean Positioning Error (cm)	STD of Error	Coefficient of Determination ( $R^2$ )
MLP Decomposition	7.68	9.38	0.98
MLP	8.98	9.29	0.98
Linear Regression	13.35	13.54	0.96
Ridge Regression	13.35	13.54	0.96
SVR-1	21.00	11.82	0.94
SVR-2	20.06	12.28	0.94
SVR-3	24.38	12.20	0.92
SVR-4	19.26	13.21	0.94
Least Squares Method	21.19	18.09	0.94

In Table II, first, we see that the MLP-based techniques outperform Linear Regression, Ridge Regression, SVR and the Least Squares Method significantly. Second, we see that the MLP Decomposition architecture outperforms all of the other techniques under examination (including the MLP) with respect to the mean positioning error. Furthermore, the standard deviation of the positioning error of the MLP Decomposition is comparable to the one for the MLP and is among the lowest two across all of the techniques. Finally, the  $R^2$  coefficient of the MLP Decomposition architecture achieves the highest value among all of the techniques and is equal to only that of the MLP.

In this table, we see that the MLP Decomposition improves the mean positioning error from 8.98 cm to 7.68 cm, compared with the MLP. Thus, not only is the MLP Decomposition a modular architecture, but also it achieves a reduction in mean positioning error of 14.5% with respect to that of the MLP. This improvement is significant given the competitive landscape of current indoor positioning techniques.

### D. Detailed Results on the MLP Decomposition Architecture

In this section, we present more detailed results on the MLP Decomposition architecture by focusing on a single test set.

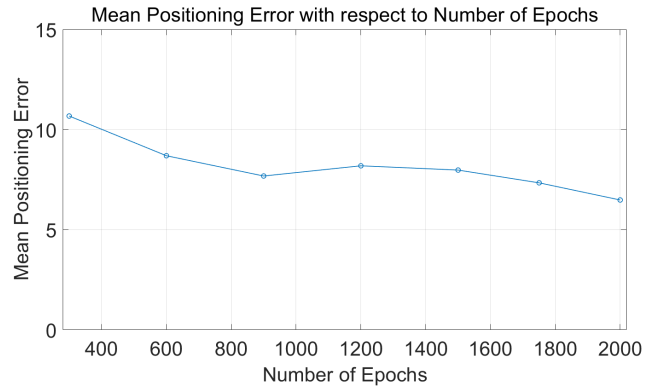


Fig. 2. Mean positioning error with respect to the number of epochs in training the MLP Decomposition model.

In Fig. 2, we display the mean positioning error with respect to the number of epochs in training the MLP Decomposition architecture. We see that the mean positioning error decreases until it reaches a cusp at 900 epochs, after which it remains relatively constant until 1500 epochs. Thus, we have decided to terminate training at 900 epochs.

Fig. 3 shows the Cumulative Distribution Function (CDF) of the positioning error under the MLP Decomposition model. We see that 48.03% of the positioning errors are within 5 cm; 84.94% are within 10 cm; and 98.03% are within 30 cm.

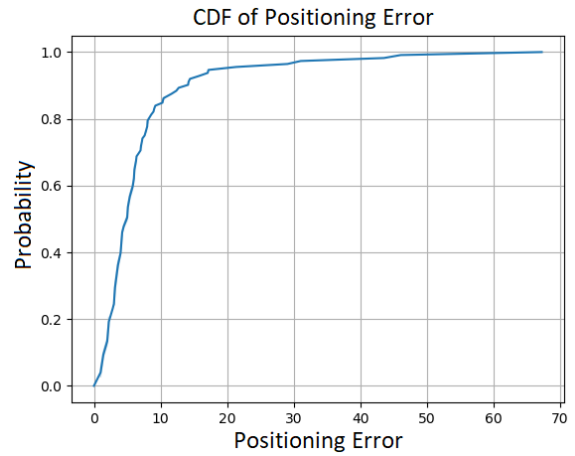


Fig. 3. The CDF of positioning error for MLP Decomposition model.

Finally, we note that for this particular test set, the training time was 146 seconds (for 900 epochs) and the execution time was 0.086 seconds for the MLP Decomposition architecture. We also found that these values were representative of the results across all of the test sets.

## V. CONCLUSION

We have developed a novel Artificial Intelligence based processing architecture, which we call the ‘‘Multi-Layer Perceptron (MLP) Decomposition architecture’’, for indoor positioning of mobile IoT devices. Our architecture takes the positions of the anchors as well as the measured distance between each anchor and the mobile IoT device as inputs and produces the estimated position of the tag.

We have measured the performance of our architecture in a demonstration in which ultra-wideband (UWB) is used as the underlying technology by virtue of which the distance to each anchor is measured. We have found that our MLP Decomposition architecture outperforms all of the following techniques in mean positioning error: MLP, Linear Regression, Ridge Regression, Support Vector Regression, and the Least Squares Method for indoor positioning. In particular, we have found in our cross-validated results that our architecture reduces the positioning error by 14.5% with respect to the MLP, which gives the second-best performance. This improvement is significant given the current competitive landscape of indoor positioning techniques.

While we have demonstrated our results only for UWB in this paper, the processing architecture that we have developed for indoor positioning is general and can be applied to any positioning technology that provides a measurement of the distance from the mobile IoT device to each anchor. Our MLP Decomposition architecture holds promise for ultra-high-precision next-generation indoor positioning of mobile IoT devices in order to enable applications such as navigation, proximity marketing, asset tracking, collision avoidance, and social distancing.

## VI. ACKNOWLEDGMENTS

The industry sponsor for the TUBITAK 2209-B grant that funded this work was SADELABS (SADE Teknoloji, Inc.), Izmir, Turkey.

## REFERENCES

- [1] F. Zafari, A. Gkelias, and K. K. Leung, "A survey of indoor localization systems and technologies," *IEEE Communications Surveys & Tutorials*, vol. 21, no. 3, pp. 2568–2599, 2019.
- [2] H. Liu, H. Darabi, P. Banerjee, and J. Liu, "Survey of wireless indoor positioning techniques and systems," *IEEE Transactions on Systems, Man, and Cybernetics, Part C (Applications and Reviews)*, vol. 37, no. 6, pp. 1067–1080, 2007.
- [3] A. Nessa, B. Adhikari, F. Hussain, and X. N. Fernando, "A survey of machine learning for indoor positioning," *IEEE Access*, vol. 8, pp. 214 945–214 965, 2020.
- [4] B. Eikens and M. Nazmulkarim, "Process identification with multiple neural network models," *International Journal of Control*, vol. 72, no. 7-8, pp. 576–590, 1999.
- [5] D. H. Wolpert, "Stacked generalization," *Neural networks*, vol. 5, no. 2, pp. 241–259, 1992.
- [6] G. Yu and H. Yan, "A new decision making method for product development based on multiple neural network," in *2006 6th World Congress on Intelligent Control and Automation*, vol. 2. IEEE, 2006, pp. 6792–6795.
- [7] J. Yang, Y. Li, and W. Cheng, "An improved geometric algorithm for indoor localization," *International Journal of Distributed Sensor Networks*, vol. 14, no. 3, p. 1550147718767376, 2018.
- [8] P. Sthapit, H.-S. Gang, and J.-Y. Pyun, "Bluetooth based indoor positioning using machine learning algorithms," in *2018 IEEE International Conference on Consumer Electronics-Asia (ICCE-Asia)*. IEEE, 2018, pp. 206–212.
- [9] Y. Dobrev, C. Reustle, T. Pavlenko, F. Cordes, and M. Vossiek, "Mobile robot 6D pose estimation using a wireless localization network," in *2016 IEEE MTT-S International Conference on Microwaves for Intelligent Mobility (ICMIM)*. IEEE, 2016, pp. 1–4.
- [10] P. Lazik and A. Rowe, "Indoor pseudo-ranging of mobile devices using ultrasonic chirps," in *Proceedings of the 10th ACM Conference on Embedded Network Sensor Systems*, 2012, pp. 99–112.
- [11] C. Sánchez, P. Taddei, S. Ceriani, E. Wolfart, and V. Sequeira, "Localization and tracking in known large environments using portable real-time 3D sensors," *Computer Vision and Image Understanding*, vol. 149, pp. 197–208, 2016.
- [12] "Leica Pegasus: Backpack wearable mobile mapping solution. [online]. Available: <http://leica-geosystems.com/products/mobile-sensor-platforms/captureplatforms/leica-pegasus-backpack>," 201.
- [13] "Realearth. [online]. Available: [www.realearth.us](http://www.realearth.us)."
- [14] D. Lymberopoulos and J. Liu, "The Microsoft Indoor Localization Competition: Experiences and lessons learned," *IEEE Signal Processing Magazine*, vol. 34, no. 5, pp. 125–140, 2017.
- [15] R. Zhang, W.-D. Zhong, Q. Kemao, and S. Zhang, "A single LED positioning system based on circle projection," *IEEE Photonics Journal*, vol. 9, no. 4, pp. 1–9, 2017.
- [16] J. Fang, Z. Yang, S. Long, Z. Wu, X. Zhao, F. Liang, Z. L. Jiang, and Z. Chen, "High-speed indoor navigation system based on Visible Light and mobile phone," *IEEE Photonics Journal*, vol. 9, no. 2, pp. 1–11, 2017.
- [17] W. Guan, S. Chen, S. Wen, Z. Tan, H. Song, and W. Hou, "High-accuracy robot indoor localization scheme based on robot operating system using Visible Light Positioning," *IEEE Photonics Journal*, vol. 12, no. 2, pp. 1–16, 2020.
- [18] S. Chen, W. Guan, Z. Tan, S. Wen, M. Liu, J. Wang, and J. Li, "High accuracy and error analysis of indoor Visible Light Positioning algorithm based on image sensor," 2020.
- [19] Y.-H. Ho, G.-H. Hou, M.-H. Wu, F.-H. Chen, P.-S. Sung, C.-H. Chen, and C.-L. Lin, "High-precision UWB indoor positioning system for customer pathway tracking," in *2019 IEEE 8th Global Conference on Consumer Electronics (GCCE)*. IEEE, 2019, pp. 466–467.
- [20] S. Li, Z. Deng, Y. Liu, and E. Hu, "A novel simultaneous calibration and localization algorithm framework for indoor scenarios," *IEEE Access*, vol. 8, pp. 180 100–180 112, 2020.
- [21] Y. Xu, G. Tian, and X. Chen, "Enhancing INS/UWB integrated position estimation using federated EFIR filtering," *IEEE Access*, vol. 6, pp. 64 461–64 469, 2018.
- [22] Y. Xu, Y. S. Shmaliy, Y. Li, and X. Chen, "UWB-based indoor human localization with time-delayed data using EFIR filtering," *IEEE Access*, vol. 5, pp. 16 676–16 683, 2017.
- [23] "Quantitec Intranav. [online]. Available: <https://intranav.com>."
- [24] A. D. P. Beuchat, H. Hesse, T. Kaufmann, R. Smith, and J. Lygeros, "UWB-based indoor localization. microsoft indoor localization competition, tech. rep. [online]. Available: <https://www.microsoft.com/en-us/research/wp-content/uploads/2016/11/beuchat.pdf>," 2017.
- [25] R. Battiti, A. Villani, and T. Le Nhat, "Neural network models for intelligent networks: deriving the location from signal patterns," *Proceedings of AINS*, 2002.
- [26] G. Ding, P. Chen, J. Tian, and Q. Zhao, "Asynchronous tracking system based on multi-path profile fingerprinting and particle filter," pp. 1–5, 2016.
- [27] A. Sashida, D. P. Moussa, M. Nakamura, and H. Kinjo, "A machine learning approach to indoor positioning for mobile targets using BLE signals," in *2019 34th International Technical Conference on Circuits/Systems, Computers and Communications (ITC-CSCC)*, 2019, pp. 1–4.
- [28] C. Jiang, J. Shen, S. Chen, Y. Chen, D. Liu, and Y. Bo, "UWB NLOS/LOS classification using deep learning method," *IEEE Communications Letters*, pp. 1–1, 2020.
- [29] S. Bozkurt, G. Elibol, S. Gunal, and U. Yayan, "A comparative study on machine learning algorithms for indoor positioning," in *2015 International Symposium on Innovations in Intelligent Systems and Applications (INISTA)*, 2015, pp. 1–8.
- [30] Z. Wu, K. Fu, E. Jedari, S. R. Shuvra, R. Rashidzadeh, and M. Saif, "A fast and resource efficient method for indoor positioning using received signal strength," *IEEE Transactions on Vehicular Technology*, vol. 65, no. 12, pp. 9747–9758, 2016.
- [31] "DWM1001 development board," Aug 2019. [Online]. Available: <https://www.decawave.com/product/dwm1001-development-board/>